American Mineralogist, Volume 72, pages 76–81, 1987

Calibration of the graphite-methane buffer using the f_{H_2} sensors at 2-kbar pressure

I-Ming Chou
959 National Center, U.S. Geological Survey, Reston, Virginia 22092, U.S.A.

Abstract

H_2 fugacities for the graphite-methane buffer assemblage in cold-seal pressure vessels have been measured at 2-kbar total pressure between 600 and 800°C using the Ag-AgBr-HBr and Ag-AgCl-HCl f_{H_2} sensors with the previously calibrated Co-CoO-H_2O buffer as a reference. The measured H_2 fugacities of the buffer at temperatures between 650 and 800°C can be represented by

$$\log (f_{H_2})_{2\ \text{kbar},T} (\pm 0.03) = 3.541 - 1675.9/T,$$

where T is in kelvins. These f_{H_2} values are about ¼ to ⅓ of the equilibrium values calculated from thermochemical data. These discrepancies may be attributed to the possibility that the H_2 fugacities generated in the pressure vessels from the decomposition of methane are not equilibrium values. However, it is also possible that the discrepancies were caused by errors in the thermochemical data and in the estimated fugacity coefficients of H_2 and CH_4 used in the equilibrium calculations. At temperatures below 650°C, reproducible steady-state f_{H_2} values may not be established, and, therefore, this buffer technique should not be used. Also, in every laboratory, this buffer must be calibrated before it is applied to mineral-stability studies because the actual H_2 fugacities for this buffer may be system-dependent.

Introduction

The assemblage graphite + methane was first suggested by Eugster and Skippen (1967) as a possible H_2 buffer and has been used to study redox reaction equilibria by Skippen (1967), Rutherford (1969, 1973), Munoz and Ludington (1974), Hallam and Eugster (1976), and Popp et al. (1976). In these studies, samples were sealed in Pt or Ag-Pd capsules, which were permeable to H_2, and a constant H_2 fugacity was superimposed on these samples at constant pressure and temperature in a cold-seal pressure vessel by equilibrating the pressure-medium CH_4 with a graphite filler rod through the reaction

$$C_{(s)} + 2H_{2(g)} = CH_{4(g)}. \quad (1)$$

The hydrogen fugacity values tabulated as a function of pressure and temperature by Skippen (1967, his Table 2) and Eugster and Skippen (1967, their Table 1) are calculated from thermochemical data. They extend from slightly higher than that of the fayalite-magnetite-quartz-H_2O buffer at 450°C to that of the wüstite-magnetite-H_2O buffer at 825°C (see Rutherford, 1969, his Fig. 3; Eugster and Skippen, 1967, their Table 1). Applications of the graphite-methane buffer technique and also of its variations have been described by Huebner (1971).

Despite the wide application of the graphite-methane buffer in the past two decades, its H_2 fugacities have never been calibrated experimentally. In this study, the graphite-methane buffer was calibrated against the Co-CoO-H_2O buffer by using the f_{H_2} sensor at 2 kbar and between 600 and 800°C. Preliminary results were presented earlier (Chou, 1980).

Experimental procedure

Preparation of f_{H_2} sensors

The f_{H_2} sensors consisted of sealed Pt capsules (1.85-mm OD, 1.54-mm ID, and 19-mm length) containing ~20-mg Ag, ~20-mg AgBr, and 15 to 20 μL of either distilled water (sensor A) or 1.5 M (molarity) HBr (sensor B). Details on the preparation, theory, and applications of a similar type of sensor, the Ag-AgCl-HCl type, have been presented elsewhere (Chou, 1978, 1987). Some sensors of the Ag-AgCl-HCl type were also used in this study to provide an independent check.

Experimental setup and sample analysis

The experimental setup is shown schematically in Figure 1. Each run consisted of four sensor capsules sealed, together with a graphite filler rod, in a conventional cold-seal pressure vessel (Tuttle, 1949). The pressure vessels were 3.18 cm in OD, 20.32 cm long, with a 6.35-mm bore, and were fabricated from Stellite 25 alloy.[1] Matheson purity methane (≧99.99% CH_4) was used as a pressure medium. To calibrate the graphite-methane buffer against the Co-CoO-H_2O buffer and to assure the attainment of osmotic equilibrium, one sensor of type A and one of type B were exposed directly to the H_2-CH_4 atmosphere of the vessel, and one each of the types A and B sensors were enclosed in separated Au capsules (3.10-mm OD, 2.70-mm ID, and 25.4-

[1] Registered trademark of Haynes Stellite Co. Use of trade names in this publication is for descriptive purpose only and does not constitute endorsement by the U.S. Geological Survey.

0003–004X/87/0102–0076$02.00

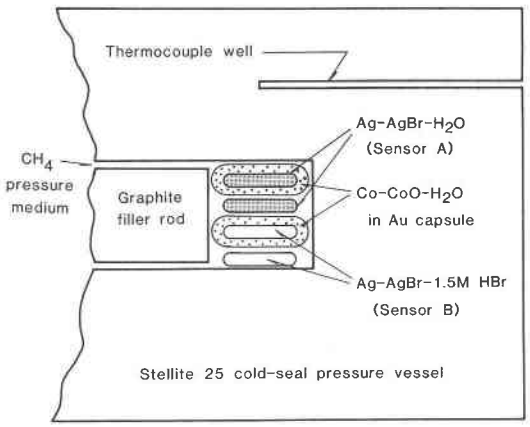

Fig. 1. Schematic diagram (not to scale) of the experimental setup.

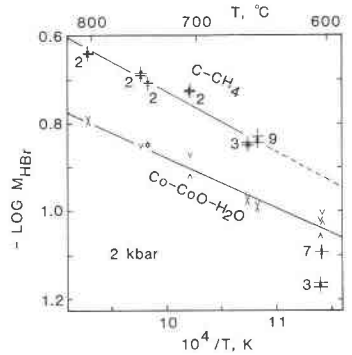

Fig. 2. Experimental results from the Ag-AgBr-HBr sensors. Plotted are the data from Table 1. The arrows and chevrons represent data from sensors exposed to the graphite-methane buffer and the Co-CoO-H_2O buffer, respectively. Data from sensors A and B are represented by the symbols pointing up and down, respectively. Uncertainties are ± 0.015 in log M_{HBr} and ± 5°C (shown by the lengths of the arrows and the horizontal bars; those associated with the chevrons are not shown for clarity). Experimental durations in days are given beside the arrows. Note that data for the Co-CoO-H_2O buffer are linear in the studied temperature range, but those for the graphite-methane buffer are linear only at higher temperatures. Lines drawn are least-squares fit of the data, excluding those at 600°C for the graphite-methane buffer. Note that data points for the graphite-methane buffer at 600°C are lower in M_{HBr} than those for the Co-CoO-H_2O buffer.

mm length) containing the Co-CoO-H_2O H_2 buffer assemblage. Combining the sample (graphite-methane buffer) and the reference (Co-CoO-H_2O buffer) runs together in a single P-T experiment not only saves time and effort but also tends to cancel out any systematic errors in measurements of pressure and temperature. After pressurization and leak test, the pressure vessel–sample assemblage was heated in a horizontal tube furnace. Furnace temperatures were regulated by means of a solid-state temperature controller, and sample temperatures were measured by a conventional potentiometer using sheathed chromel-alumel thermocouples, which were calibrated against the melting points of NaCl (800.6°C), KCl (769.9°C), Al (659.9°C), and Zn (419.5°C) at 1 atm. The reported temperatures are estimated to be accurate to within ± 5°C. A Heise gauge was used to monitor the pressure. Because the H_2 produced by the decomposition of CH_4 leaked continuously through the wall of the pressure vessel, CH_4 had to be replenished from time to time to maintain the total pressure. The maximum pressure drop was about 35 bars.

At the conclusion of each equilibration period, the pressure vessel–sample assemblage was quenched by a stream of compressed air. Capsules were removed, cleaned, and weighed. The sensor capsules were cleaned and pierced on a Teflon plate with a tungsten carbide needle. Between 5 and 10 μL of the solution were removed using a microcapacity disposable pipet, and bromide or chloride contents were then determined coulometrically with a Buchler Digital chloridometer. To ascertain that all solid buffer phases were present, the buffers were examined optically and/or by X-ray diffraction. In order to identify the nature of

Table 1. Experimental results from the Ag-AgBr-HBr hydrogen sensors at 2 kbar

Run no.	Pressure vessel no.	T (°C)	Duration (d)	Buffer	M_{Br^-}*	Log M_{Br^-}
17	15	804	2	Co-CoO	0.1613, 0.1611	−0.792, −0.793
				C-CH_4	0.2293, 0.2276	−0.640, −0.643
16	13	751	2	Co-CoO	—**, 0.1396	—**, −0.857
				C-CH_4	0.2042, 0.2065	−0.690, −0.685
18	13	744	2	Co-CoO	0.1445, 0.1384	−0.840, −0.859
				C-CH_4	0.1961, 0.1968	−0.708, −0.706
14	13	706	2	Co-CoO	0.1224, 0.1316	−0.912, −0.881
				C-CH_4	0.1869, 0.1881	−0.728, −0.726
12	13	658	3	Co-CoO	0.1061, 0.1058	−0.974, −0.976
				C-CH_4	0.1426, 0.1411	−0.846, −0.851
9	13	650	9	Co-CoO	0.1018, 0.1016	−0.992, −0.993
				C-CH_4	0.1474, 0.1428	−0.832, −0.845
11	15	604	3	Co-CoO	0.0888, 0.0941	−1.052, −1.026
				C-CH_4	0.0685, 0.0670	−1.164, −1.174
15	15	603	7	Co-CoO	0.0956, 0.0968	−1.020, −1.014
				C-CH_4	0.0802, 0.0808	−1.096, −1.093

* Molarities of Br^- measured coulometrically by a chloridometer. Two numbers are given for each buffer in each run; the first for sensor A and the second for sensor B.

** Sensor A leaked.

Table 2. f_{H_2} values for the C-CH_4 buffer calibrated against those of the Co-CoO-H_2O buffer at 2-kbar total pressure

Run no.	T (°C)	Log $(f_{O_2})^{Co\text{-}CoO}$ *	Log K_w **	Log f_{H_2O} ‡	Log $(f_{H_2})^{Co\text{-}CoO}$ †	Log $(f_{H_2})^{C\text{-}CH_4}$ ††	$(f_{H_2})^{C\text{-}CH_4}$ (bars)
17	804	−15.205	9.131	3.200	1.671	1.974	94.194
16	751	−16.364	9.754	3.167	1.595	1.930	85.201
18	744	−16.527	9.841	3.162	1.584	1.869	74.033
14	706	−17.448	10.335	3.133	1.521	1.861	72.630
12	658	−18.719	11.016	3.088	1.431	1.685	48.373
9	650	−18.943	11.136	3.079	1.415	1.724	52.913
11	604	−20.314	11.870	3.025	1.312	1.052	11.260
15	603	−20.346	11.887	3.023	1.310	1.155	14.291

* Calculated from $\log (f_{O_2})^{Co\text{-}CoO} = -24\,242.6/T + 7.205 + 0.052(P - 1)/T$, where T is temperature in kelvins, and P is pressure in bars (Chou, 1987).
** Equilibrium constant for the reaction $H_2 + \frac{1}{2}O_2 = H_2O$; interpolated from Robie et al. (1979).
‡ Interpolated from Burnham et al. (1969).
† Calculated from $\log f_{H_2} = \log f_{H_2O} - \log K_w - \frac{1}{2}\log f_{O_2}$.
†† Calculated from Eq. 10; average values of M_{Br^-} from sensors A and B for each buffer were used in the calculation.

carbon produced by the decomposition of methane (Reaction 1) and also to study the possible interactions between the pressure vessel and the graphite-methane buffer system, the precipitates in the pressure vessels were also examined.

Experimental result

The experimental results from the Ag-AgBr-HBr sensors are given in Table 1 and plotted in Figure 2. Hydrogen fugacities for the graphite-methane buffer calculated from these data are tabulated in Table 2. Results from the Ag-AgCl-HCl sensors are given in Table 3.

Calculations of hydrogen fugacities

For the reaction in the Ag-AgBr-HBr sensors at fixed P, and T, assuming pure solid Ag,

$$Ag_{(s)} + HBr_{(g)} = AgBr_{(l)} + \tfrac{1}{2}H_{2(g)} \quad (2)$$

$$(K_2)_{P,T} = f_{H_2}^{1/2} a_{AgBr}/f_{HBr}, \quad (3)$$

where a_{AgBr} is the activity of AgBr in the liquid AgBr phase, and f_{HBr} is the fugacity of HBr in the gas mixture at P and T. Also,

$$f_{HBr} = f^*_{HBr} X_{HBr} \lambda_{HBr}, \quad (4)$$

where f^*_{HBr} is the fugacity of pure HBr at the same P and T, λ_{HBr} is the activity coefficient of HBr in the mixture at P and T using pure HBr at the same P and T as the standard state, and X_{HBr} is the mole fraction of HBr in the mixture

Table 3. Experimental results and calibration of f_{H_2} from the Ag-AgCl-HCl hydrogen sensors at 2 kbar

Run no.	Pressure vessel no.	T (°C)	Duration (d)	Buffer	M_{Cl^-} *	m_{Cl^-} **	Log $(f_{H_2})^{C\text{-}CH_4}$ ‡
7	13	653	6	Co-CoO	(A) 1.543, 1.545	1.593	—
					(B) 1.580, 1.601	1.643	—
				C-CH_4	(A) 2.183, 2.181	2.281	1.722
					(B) 2.096, 2.080	2.179	1.682
5	13	651	1	Co-CoO	(A) 1.259	1.292	—
				C-CH_4	(A) 1.897	1.972	1.786
					(B) 1.885	1.959	1.781
3	13	650	3	C-CH_4	(A) 1.802, 1.824	1.881	1.745
					(B) 1.781, 1.772	1.842	1.727
6	15	605	1	Co-CoO	(A) 1.001, 1.024	1.034	—
				C-CH_4	(A) 1.254, 1.258	1.289	1.509
					(B) 1.263, 1.265	1.297	1.514
8	15	604	6	Co-CoO	(A) 1.014, 1.028	1.043	—
					(B) 0.998, 0.985	1.012	—
				C-CH_4	(A) 1.300, 1.314	1.343	1.545
					(B) 1.282, 1.295	1.323	1.532
4	15	600	3	Co-CoO	(A) 0.969, 0.961	0.984	—
				C-CH_4	(A) 1.265, 1.279	1.306	1.551
					(B) 1.263, 1.267	1.299	1.546

* For sensors A and B as indicated; sensor B was not used in some runs.
** Molalities were calculated from Eq. 12; average values.
‡ Calculated from Eq. 13; in run no. 3, Co-CoO-H_2O buffer was not used and $m_{Cl^-}^{Co\text{-}CoO} = 1.292$ from run no. 5 was used in the calculation.

$$X_{HBr} = m_{HBr}/(m_{H_2O} + m_{HBr} + m_{H_2} + m_{Br_2} + m_{O_2}), \quad (5)$$

where m_i is molality of i at P and T.

Combining Equations 3, 4, and 5, we have

$$(f_{H_2})_{P,T} = [(K_2 f^*_{HBr}\lambda_{HBr})/(a_{AgBr}\Sigma m_i)]^2_{P,T}(m_{HBr})^2_{P,T}, \quad (6)$$

where i includes H_2O, HBr, H_2, Br_2, and O_2, and m_{HBr} is the molality of associated HBr at P and T. At 2-kbar total pressure, according to the ionization-constant data of HBr (Quist and Marshall, 1968), more than 91% and 97% of total Br ($m_{HBr} + m_{Br^-}$) at, respectively, 600 and 650°C are associated. Therefore,

$$(m_{Br^-})_{1\ atm,25°C} = (m_{HBr} + m_{Br^-})_{P,T} \simeq (m_{HBr})_{P,T}, \quad (7)$$

where $(m_{Br^-})_{1\ atm,25°C}$ is the total molality of Br^- at 1 atm and 25°C and is assumed to be the same as the molarity (M) of Br^- measured after quench. Because the HBr solutions in this study are so dilute (<0.23 M) that

$$(m_{Br^-})_{1\ atm,25°C} \approx (M_{Br^-})_{1\ atm,25°C}. \quad (8)$$

Combining Equations 6, 7, and 8, we have

$$(f_{H_2})_{P,T} = [(K_2 f^*_{HBr}\lambda_{HBr})/(a_{AgBr}\Sigma m_i)]^2_{P,T}(M_{Br^-})^2_{1\ atm,25°C}. \quad (9)$$

Osmotic equilibrium can be demonstrated by attaining reversibility in the flow of H_2 (Shaw, 1967, p. 529). As the system approaches equilibrium, H_2 in the outer system diffuses into sensor A and reacts with AgBr forming HBr, while HBr in sensor B reacts with Ag producing AgBr and H_2, which diffuses out of sensor B into the outer system. The same value for $(M_{Br^-})_{1\ atm,25°C}$ in sensors A and B in each run indicates that the system has reached osmotic equilibrium, and the $(f_{H_2})_{P,T}$ obtained from the $(M_{Br^-})_{1\ atm,25°C}$ value measured in the sensors and calculated from Equation 9 reflects f_{H_2} of the outer system. Two kinds of outer systems were used in this study to superimpose constant f_{H_2} values in each run: one by the graphite-methane (C-CH_4) buffer and the other by the Co-CoO-H_2O buffer (see Fig. 1). According to Equation 9, these two f_{H_2} values are related by

$$(f_{H_2})^{C\text{-}CH_4} = (f_{H_2})^{Co\text{-}CoO}_{P,T}(M^{C\text{-}CH_4}_{Br^-}/M^{Co\text{-}CoO}_{Br^-})^2_{1\ atm,25°C}, \quad (10)$$

assuming

$$[\lambda_{HBr}/(a_{AgBr}\Sigma m_i)]^{C\text{-}CH_4}_{P,T} = [\lambda_{HBr}/(a_{AgBr}\Sigma m_i)]^{Co\text{-}CoO}_{P,T}, \quad (11)$$

which is a reasonable assumption because the gas compositions in the sensors exposed to these two buffer systems are not very different.

The $(f_{H_2})^{C\text{-}CH_4}_{P,T}$ values calculated from Equation 10 and the $(M_{Br^-})_{1\ atm,25°C}$ data given in Table 1 are listed in Table 2 and plotted in Figure 3 (open boxes). The calculations of $(f_{H_2})_{P,T}$ are also given in Table 2. The Co-CoO buffer has been calibrated against the Ni-NiO buffer by using the same technique (Chou, 1978, 1987), and the f_{O_2} values of the Co-CoO buffer reported by Chou (1987) are adopted here.

Procedures for calculating $(f_{H_2})^{C\text{-}Ch_4}$ from the Ag-AgCl-HCl sensor experiments are the same as those described above for the Ag-AgBr-HBr sensors, except that the equivalent approximation of Equation 8 has to be modified (Chou, 1987) by

$$m_{Cl^-} = 4.67 \times 10^{-4} + 0.99962\, M_{Cl^-} + 0.02087\, M^2_{Cl^-} \quad (12)$$

because molality and molarity units for a concentrated Cl^- solution are somewhat different, as shown in Table 3. Consequently, Equation 10 becomes

$$(f_{H_2})^{C\text{-}CH_4}_{P,T} = (f_{H_2})^{Co\text{-}CoO}_{P,T}(m^{C\text{-}CH_4}_{Cl^-}/m^{Co\text{-}CoO}_{Cl^-})^2_{1\ atm,25°C}. \quad (13)$$

Results are given in Table 3 and plotted in Figure 3 (shaded boxes).

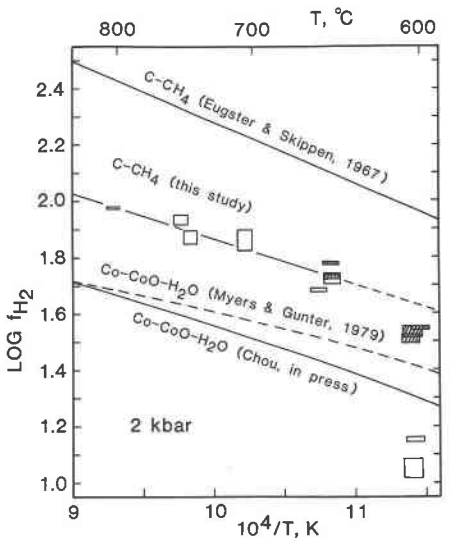

Fig. 3. H_2 fugacities of the graphite-methane buffer calibrated by means of the Ag-AgBr-HBr sensors (open boxes) and by means of the Ag-AgCl-HCl sensors (shaded boxes). Note that the two open boxes at 600°C are below 1.2 in $\log f_{H_2}$. Uncertainties are indicated by the size of the box. The line indicated by C-CH_4 (this study) is the least-squares fit of the data above 650°C. H_2 fugacities for the buffer at 600°C are not reproducible (for details, see text). Also shown for comparison are H_2 fugacities of the Co-CoO-H_2O buffer calculated from the f_{O_2} data of Chou (1987) and from those of Myers and Gunter (1979), and the equilibrium f_{H_2} for the graphite-methane buffer calculated from thermochemical data (Eugster and Skippen, 1967).

Discussion

H_2 fugacities of the graphite-methane buffer measured by means of the Ag-AgBr-HBr and Ag-AgCl-HCl sensors at temperatures between 650 and 804°C can be represented by the equation

$$\log (f_{H_2})^{C\text{-}CH_4}_{2\ kbar,T}\ (\pm 0.03) = 3.541 - 1675.9/T \quad (14)$$

where T is temperature in kelvins. Equation 14 is the least-squares fit of the data given in Tables 2 and 3, and is shown in Figure 3. The coefficient of determination $r^2 = 0.890$. These measured H_2 fugacities are about ⅓ to ¼ of the equilibrium values calculated from thermochemical data (Eugster and Skippen, 1967). These discrepancies are too large to be totally attributed to the uncertainties associated with the Co-CoO buffer; when the Co-CoO

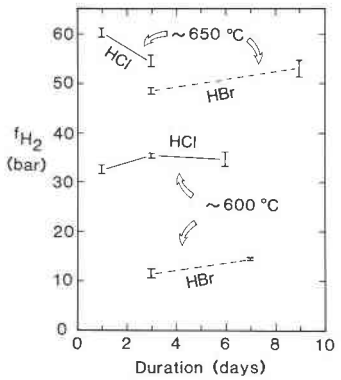

Fig. 4. Variations of f_{H_2} for the graphite-methane buffer as a function of experimental duration at ~650 and ~600°C measured by the Ag-AgBr-HBr sensors (dashed lines) and by the Ag-AgCl-HCl sensors (solid lines). (For discussion, see text.)

buffer data reported by Myers and Gunter (1979) (also Fig. 3) are used in Equations 10 and 13, the $(f_{H_2})^{C\text{-}CH_4}$ values reported in Table 2 are only, respectively, 4.48, 10.56, and 3.26 bars higher at 804, 706, and 604°C. However, the discrepancies between the calculated and the measured H_2 fugacities may be attributed to (1) the errors in the thermochemical data and in the estimated fugacity coefficients of H_2 and CH_4 used in the calculations, and/or (2) the nonequilibrium nature of the measured H_2 fugacities. The reasons for (2) are (a) the buffer reaction (Eq. 1) was calibrated in the direction of H_2 generation only, and the reversal of the reaction was not demonstrated; (b) the X-ray diffraction data show that carbon produced by the decomposition of methane was amorphous instead of crystalline graphite (the former had a higher carbon activity that resulted in a lower f_{H_2}, as observed); (c) a continuous leakage of H_2 from the pressure vessels was indicated by the continuous total pressure drop during the run; and (d) the buffer system was contaminated by the pressure-vessel material as indicted by the presence of Ni_xC ($x > 4$) and WC as reaction products. Ni_xC and WC were examined optically and by means of the X-ray diffraction. Ni_xC was identified by its (111), (200), and (022) peaks (Pugh et al., 1961), and WC by its (001), (100), and (101) peaks (Goldschmidt, 1949). Ni and W came from the Stellite 25 pressure vessels, which consisted mainly of Co (~50–55 wt%), Cr (~20%), W (~15%), Ni (~10%), and Fe ($\lesssim$3%).

Even though equilibrium H_2 fugacities for the graphite-methane buffer may not be obtained in the pressure vessels, steady-state values can be established through two counteracting processes: steady generation of H_2 by decomposition of methane and steady loss of H_2 by diffusion through the pressure vessel wall. The f_{H_2} values measured by using the Ag-AgCl-HCl and Ag-AgBr-HBr sensors at 2-kbar total pressure and at ~650 and ~600°C are compared in Figure 4 as a function of experimental duration. In order to minimize the difference in their physical setup, the same pressure vessel–furnace assembly was used for all runs in each temperature set. At ~650°C, f_{H_2} values of the graphite-methane buffer measured by means of the two types of sensors converge in about 3 d. Those at ~600°C do not converge at all, even though each system where the same kinds of sensors are used tends to establish its own quasi-steady-state f_{H_2}; the quasi-steady-state f_{H_2} values measured by the Ag-AgCl-HCl sensors are more than two times higher than those determined by the Ag-AgBr-HBr sensors. This discrepancy cannot be attributed to the uncertainties in pressure, temperature, and chemical analysis, because each run has its own Co-CoO-H_2O buffer reference, which behaves normally as indicated by the linear relation of the data in the log M_{Br^-} vs. $1/T$ plot shown in Figure 2. However, it is possible that at ~600°C, the rate of H_2 generation in Reaction 1 is so sluggish that the steady-state f_{H_2} of the system is not controlled by this reaction but rather by the budget of H_2 in the system, with the sensors attempting to control f_{H_2}. The other H_2-generating reaction in the system is in sensor B (see Eq. 2). The difference in the steady-state f_{H_2} measured by the two types of sensors shown in Figure 4 is then the result of the difference in their initial acid concentrations in the B sensors (i.e., 3.0 *M* HCl vs. 1.5 *M* HBr).

Because the steady-state H_2 fugacities approximated by Equation 14 may not be the equilibrium values for the graphite-methane buffer, and also because the permeation rates of H_2 through the pressure-vessel walls depend on the material, dimension, and history of usage of the pressure vessels, this buffer must be calibrated in every laboratory before it can be applied in redox-controlled studies. Also, the graphite-methane buffer should not be used at temperatures below 650°C, because reproducible steady-state H_2 fugacities may not be established at these low temperatures.

Conclusions

The H_2 fugacities for the graphite-methane buffer have been calibrated at 2-kbar total pressure against the previously calibrated Co-CoO-H_2O buffer between 600 and 800°C. At temperatures below 650°C, reproducible steady-state f_{H_2} may not be established, probably because of the sluggish nature of the decomposition reaction of CH_4 in Reaction 1. However, at higher temperatures, steady-state f_{H_2} can be established and maintained. The graphite-methane buffer must be calibrated in every laboratory before it can be used in mineral stability studies, because the steady-state f_{H_2} values approximated from Equation 14 may not represent equilibrium values and the actual f_{H_2} values of this buffer may be system-dependent.

Note added in proof. The discrepancies between the calculated and measured f_{H_2} values for the C-CH_4 buffer (see Fig. 3) can be partially attributed to the possible nonequilibrium nature of the measured M_{Br^-} and M_{Cl^-} values in the f_{H_2} sensors exposed to the Co-CoO-H_2O buffer; those concentrations listed in Tables 1 and 3 (except run nos.

11 and 15) are probably higher than their respective equilibrium values owing to the relatively high flux of H_2 into the Au capsules coupled with the sluggishness of the buffer reaction ($CoO + H_2 \rightarrow Co + H_2O$).

Acknowledgments

J. S. Huebner kindly provided access to his high-pressure equipment and X-ray facilities. Reviews by J. J. Hemley, J. R. Holloway, M. Sato, H. R. Shaw, and J. V. Walther were greatly appreciated.

References

Burnham, C.W., Holloway, J.R., and Davis, N.F. (1969) Thermodynamic properties of water to 1000°C and 10 000 bars. Geological Society of America Special Paper Number 132.

Chou, I-Ming. (1978) Calibration of oxygen buffers at elevated *P* and *T* using the hydrogen fugacity sensor. American Mineralogist, 63, 690–703.

——— (1980) Calibration of the graphite-methane buffer using the hydrogen-fugacity sensor. Geological Society of America Abstracts with Programs, 12, 402.

——— (1987) Oxygen buffer and hydrogen sensor techniques at elevated pressures and temperatures. In H.L. Barnes and G.C. Ulmer, Eds. Hydrothermal experimental techniques, in press. Wiley, New York.

Eugster, H.P., and Skippen, G.B. (1967) Igneous and metamorphic reactions involving gas equilibria. In P.H. Abelson, Ed. Researches in geochemistry, vol. 2, p. 377–396. Wiley, New York.

Goldschmidt, H.J. (1949) Interplanar spacings of carbides in steels. Metallurgia, 40, 103–104.

Hallam, M., and Eugster, H.P. (1976) Ammonium silicate stability relations. Contributions to Mineralogy and Petrology, 57, 227–244.

Huebner, J.S. (1971) Buffering techniques for hydrostatic systems at elevated pressures. In G.C. Ulmer, Ed. Research techniques for high pressure and high temperature, p. 123–177. Springer-Verlag, New York.

Munoz, J.L., and Ludington, S.D. (1974) Fluoride-hydroxyl exchange in biotite. American Journal of Science, 274, 396–413.

Myers, J., and Gunter, W.D. (1979) Measurement of the oxygen fugacity of the cobalt-cobalt oxide buffer assemblage. American Mineralogist, 64, 224–228.

Popp, R.K., Gilbert, M.C., and Craig, J.R. (1976) Synthesis and X-ray properties of Fe-Mg orthoamphiboles. American Mineralogist, 61, 1267–1279.

Pugh, H.L.D., Lees, J., and Bland, J.A. (1961) Synthesis and X-ray analysis of diamond. Nature, 191, 865–867.

Quist, A.S., and Marshall, W.L. (1968) Electrical conductances of aqueous hydrogen bromide solutions from 0 to 800° and at pressures to 4000 bars. Journal of Physical Chemistry, 72, 1545–1552.

Robie, R.A., Hemingway, B., and Fisher, J.R. (1979) Thermodynamic properties of minerals and related substances at 298.15 K and 1 bar (10^5 pascals) pressure and at higher temperatures. U.S. Geological Survey Bulletin 1452 (reprinted with corrections).

Rutherford, M.J. (1969) An experimental determination of iron biotite–alkali feldspar equilibria. Journal of Petrology, 10, 381–408.

——— (1973) The phase relations of aluminous iron biotites in the system $KAlSi_3O_8$-$KAlSiO_4$-Al_2O_3-Fe-O-H. Journal of Petrology, 14, 159–180.

Shaw, H.R. (1967) Hydrogen osmosis in hydrothermal experiments. In P.H. Abelson, Ed. Researches in geochemistry, vol. 2, p. 521–541. Wiley, New York.

Skippen, G.B. (1967) An experimental study of the metamorphism of siliceous carbonate rocks. Ph.D. thesis, Johns Hopkins University, Baltimore, Maryland.

Tuttle, O.F. (1949) Two pressure vessels for silicate-water studies. Geological Society of America Bulletin, 60, 1727–1729.

Manuscript received April 23, 1986
Manuscript accepted September 2, 1986